Protein Science (1998), 7:619–627. Cambridge University Press. Printed in the USA.

Solution structure of Compstatin, a potent complement inhibitor

DIMITRIOS MORIKIS,[1] NURIA ASSA-MUNT,[1] ARVIND SAHU,[2] AND JOHN D. LAMBRIS[2]

[1]The Burnham Institute, 10901 North Torrey Pines Road, La Jolla, California 92037
[2]Laboratory of Protein Chemistry, Department of Pathology and Laboratory Medicine, University of Pennsylvania, Philadelphia, Pennsylvania 19104

(RECEIVED August 28, 1997; ACCEPTED October 30, 1997)

Abstract

The third component of complement, C3, plays a central role in activation of the classical, alternative, and lectin pathways of complement activation. Recently, we have identified a 13-residue cyclic peptide (named Compstatin) that specifically binds to C3 and inhibits complement activation. To investigate the topology and the contribution of each critical residue to the binding of Compstatin to C3, we have now determined the solution structure using 2D NMR techniques; we have also synthesized substitution analogues and used these to study the structure–function relationships involved. Finally, we have generated an ensemble of a family of solution structures of the peptide with a hybrid distance geometry-restrained simulated-annealing methodology, using distance, dihedral angle, and $^3J_{NH\text{-}H\alpha}$-coupling constant restraints. The Compstatin structure contained a type I β-turn comprising the segment Gln^5-Asp^6-Trp^7-Gly^8. Preference for packing of the hydrophobic side chains of Val^3, Val^4, and Trp^7 was observed. The generated structure was also analyzed for consistency using NMR parameters such as NOE connectivity patterns, $^3J_{NH\text{-}H\alpha}$-coupling constants, and chemical shifts. Analysis of Ala substitution analogues suggested that Val^3, Gln^5, Asp^6, Trp^7, and Gly^8 contribute significantly to the inhibitory activity of the peptide. Substitution of Gly^8 caused a 100-fold decrease in inhibitory potency. In contrast, substitution of Val^4, His^9, His^{10}, and Arg^{11} resulted in minimal change in the activity. These findings indicate that specific side-chain interactions and the β-turn are critical for preservation of the conformational stability of Compstatin and they might be significant for maintaining the functional activity of Compstatin.

Keywords: complement; complement inhibitor; C3; NMR; peptide; structure calculation

The complement system is the first line of immunological defense against foreign pathogens (Muller-Eberhard, 1992). Its activation through the classical, alternative, or lectin pathways leads to the generation of anaphylatoxic peptides C3a and C5a and formation of the C5b-9 membrane attack complex. Complement component C3 plays a central role in activation of all three pathways. Activation of C3 by complement pathway C3 convertases and its subsequent attachment to target surface leads to assembly of the membrane attack complex and ultimately to damage or lysis of the target cells (Frank & Fries, 1991). C3 is unique in that it possesses a rich architecture that provides a multiplicity of diverse ligand binding sites that are important in immune surveillance and immune response pathways (Lambris, 1990, 1993).

Inappropriate activation of complement may lead to host cell damage. Complement is implicated in several disease states, including various autoimmune diseases, and has been found to contribute to other clinical conditions, such as adult respiratory syndrome (Robbins et al., 1987), stroke (Vasthare et al., 1993), heart attack (Kilgore et al., 1994), rejection following xenotransplantation (Wang et al., 1992), and burn injuries (Gallinaro et al., 1992). Complement-mediated tissue injury has also been found to result from bioincompatibility situations, such as those encountered in patients undergoing dialysis (Pekna et al., 1993) or cardiopulmonary bypass (Gillinov et al., 1994).

Complement-mediated tissue injuries are mediated directly by the membrane attack complex, and indirectly by the generation of C3a and C5a (Hugli, 1990; Ember et al., 1992). These peptides induce damage through their effects on neutrophils (Ehrengruber et al., 1994) and mast cells (Ellati et al., 1994). In vivo, regulation of complement at the C3 and C5 activation steps is provided by both plasma and membrane proteins. The plasma protein inhibitors are factor H and C4-binding protein, and the regulatory membrane proteins located on cell surfaces are complement receptors 1 (CR1),

Reprint requests to: John D. Lambris, Laboratory of Protein Chemistry, Department of Pathology and Laboratory Medicine, University of Pennsylvania, 410 Johnson Pavillon, Philadelphia, Pennsylvania 19104; e-mail: lambris@mail.med.upenn.edu or to: Nuria Assa-Munt, The Burnham Institute, 10901 North Torrey Pines Road, La Jolla, California 92037; e-mail: nuria@ljorf.edu.

Abbreviations: C3, third component of complement; C3b, the proteolytically activated form of C3; NHS, normal human serum; Er, rabbit erythrocytes; RMSD, RMS deviation; TFA, trifluoroacetic acid; TOCSY, total correlation spectroscopy; DQF-COSY, double quantum filtered correlated spectroscopy; DQ, double quantum spectroscopy; NOESY, NOE spectroscopy; J-R NOESY, jump-and-return NOE spectroscopy; ROESY, rotating frame NOE spectroscopy.

decay-accelerating factor (DAF), and membrane cofactor protein (MCP) (Holers et al., 1992). These proteins inhibit the C3 and C5 convertases (multisubunit proteases) by promoting dissociation of the multisubunit complexes and/or by inactivating the complexes through proteolysis (catalyzed by factor I). Several pharmacological agents that regulate or modulate complement activity have been identified by in vitro assay, but most have been shown to be of low activity or toxic (Johnson, 1977; Reynard, 1980; Kalli et al., 1994; Morgan, 1994).

Recently, we have used a phage-displayed random peptide library to identify peptides that bind C3 and inhibit complement. Using this approach, we have isolated a small cyclic inhibitory C3-binding peptide (now named Compstatin), which inactivates complement at a concentration approximately twice that of human C3 in normal human serum (Sahu et al., 1996). The experiments performed to elucidate the mechanism of complement inhibition by Compstatin suggested that this peptide reversibly binds to native C3 to inhibit its activation and that the inhibition is not a result of sterically hindered access to the C3a/C3b cleavage site (Sahu et al., 1996). Compstatin is a 13-residue cyclic peptide of 1551 Da with sequence:

$$\underset{\text{S—S}}{\text{I C V V Q D W G H H R C}}\ \text{T-NH}_2,$$

which contains a disulfide bridge between Cys^2 and Cys^{12}. Elucidation of the solution structure of free Compstatin is a first step toward understanding the topology and the mechanism of the peptide binding to C3.

Small peptides are, in most cases, present in solution as an ensemble of interconverting conformers (Dyson & Wright, 1991, 1995). In some cases, the population of one or more conformers in the ensemble can be high enough for detection by spectroscopic methods. Cyclic peptides are more restrained in flexibility compared to linear peptides, and they are more likely to demonstrate a preference for an observable conformer. The presence of rapidly interconverting conformers is reflected in the measured NMR parameters, which are population-weighted averages of the individual contributing structures.

In the present study, we have used NMR spectroscopy to extract distance, dihedral angle, and $^3J_{\text{NH-H}\alpha}$-coupling constant restraints (Wüthrich, 1986), which we have used for the structure elucidation of a major Compstatin conformer. We utilized a hybrid distance geometry-restrained simulated-annealing methodology (Nilges et al., 1988; Kuszewski et al., 1992) for the structure calculation. Subsequently, we examined the structure for consistency using characteristic NOE connectivities, $^3J_{\text{NH-H}\alpha}$-coupling constants, chemical shifts, and temperature dependence of chemical shifts (Wüthrich, 1986; Dyson et al., 1988). In addition, we analyzed the contribution of each amino acid residue by synthesizing and examining the inhibitory activity of a series of analogue peptides with Ala substitutions. The analogue data, together with the 2D NMR data, indicate that the type I β-turn segment (Gln^5-Asp^6-Trp^7-Gly^8) plays a significant role in the inhibitory activity of Compstatin.

Results and discussion

NMR assignment and restraints

Proton resonance assignments were made according to standard procedures (reviewed in Wüthrich, 1986).

Amino acid spin systems were identified by locating networks of characteristic connectivities in the 2D TOCSY spectrum at 5 °C. Figure 1 shows the assignment of all 13 spin systems of Compstatin. The NH of Ile^1 is not observable because of fast exchange with the solvent, but the rest of the spin system is shown at $\omega_2 = \omega_{\text{H}\alpha}$ (right panel of Fig. 1). In addition, the DQ spectra were very useful for resolving ambiguities and verifying the proton assignments. In particular, a remote cross peak was observed in the DQ spectrum at $\omega_2 = \omega_{\text{NH}}$ and $\omega_1 = \omega_{\text{H}\alpha 1} + \omega_{\text{H}\alpha 2}$ for Gly^8. This cross peak confirmed the assignment of the two degenerate α-protons of Gly^8 and resolved the ambiguity at $\omega_2 = \omega_{\text{NH}} = 8.47$ ppm, which is the frequency of three amide protons (Gln^5, Gly^8, Arg^{11}). Raising the temperature to 10 °C introduced small shifts in the resonances of NH protons, a change that allowed us to verify all assignments.

Inspection of the 2D NMR spectra indicated the presence of a set of cross peaks corresponding to the backbone of a single Compstatin conformation. However, some side chains, such as Gln^5 and Trp^7, indicated the presence of additional minor conformations. Measurement of the volumes of the NH^{ϵ} diagonal peaks of Trp^7 in the 2D NOESY spectrum indicated that the Trp^7 ring populated four different conformations with population of 96% for the major side-chain conformer and 4% for the rest. No inter- or intraresidue NOEs involving the minor side-chain conformations were found,

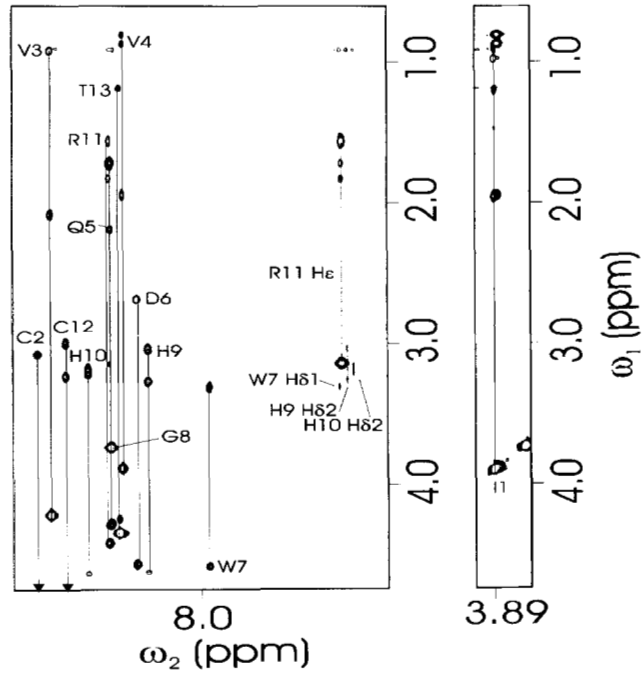

Fig. 1. A portion of the 500-MHz 2D TOCSY spectrum of Compstatin. All 13 spin systems are identified, and individual spins within the same spin system are connected with lines. The right panel shows the spin system of Ile^1 originating from the α-proton, because the NH of the first residue in the sequence is not observable due to fast exchange with the solvent. Arrows point to NH-H^{α} cross peaks of Cys^2 and Cys^{12} outside the limits of the plot. These cross peaks are very weak because their H^{α}-resonances are close to the solvent water resonance and they are attenuated by the water presaturation scheme of the data acquisition pulse sequence. However, they are present in the J-R NOESY or DQ spectra. Some TOCSY connectivities involving the Arg^{11} NH^{ϵ} and long-range couplings between aromatic and side-chain protons are also shown. Sample conditions are pH 6 and 5 °C.

and no conformational exchange cross peaks were found in the ROESY spectrum. For the rest of our analysis, we used the unique backbone cross peaks and the cross peaks of the major side-chain conformer of Gln^5 and Trp^7.

Sequence-specific and long-range NOE assignments were made using the 200- and 400-ms NOESY and the 200-ms J-R NOESY spectra collected at 5 °C and 10 °C. The J-R NOESY was particularly useful for detecting NOEs involving the α-protons of Cys^2 and Cys^{12}, which are very close to the resonance of water and are "bleached out" by the water suppression scheme of the regular NOESY pulse sequence. 2D ROESY spectra of Compstatin were used to verify the regular NOE assignments that had been made using the 2D NOESY and J-R NOESY spectra.

Structure calculations

Figure 2A shows the backbone and the disulfide bond of the ensemble of the 21 accepted final refined structures for Compstatin. A turn segment was observed in the best-defined region between residues Gln^5 and Gly^8. Figure 2B shows the backbone of the average restrained regularized structure of the ensemble for the segment Gln^5-Asp^6-Trp^7-Gly^8. The turn segment and the two valines, Val^3 and Val^4, appeared to be better defined than the rest of the peptide. This difference is due to the lack of a significant number of long-range NOE restraints outside the segment Val^3–Gly^8. The average RMSD of the ensemble of 21 structures for Compstatin was 0.6 Å for the backbone heavy atoms and 1.2 Å for all heavy atoms. The statistics for the ensemble of the family of structures and for the average regularized structure are summarized in Table 1. The program PROCHECK-NMR (Laskowski et al., 1996) was used for structure validation and analysis. We found that 90% of the residues lay in the most favored or additionally favored regions of the Ramachandran plot (Ramachandran et al., 1963) using the average restrained regularized structure of Compstatin.

Table 1. *Structural statistics for the ensemble of the family of the 21 final refined structures and the restraint regularized mean structure of Compstatin*[a]

Structural statistics	⟨*Compstatin*⟩	$(\overline{Compstatin})_r$
Experimental RMS deviations		
NOE-derived distance restraints (Å)	0.044 ± 0.003	0.053
Dihedral angle restraints (°)	0.46 ± 0.35	0.21
Deviations from idealized geometry		
Bonds (Å)	0.003 ± 0.0003	0.003
Angles (°)	0.55 ± 0.04	0.55
Improper angles (°)	0.33 ± 0.03	0.34
Potential energies (kcal mol^{-1})		
Total	38.9 ± 5.5	43.3
NOE restraints	13.0 ± 1.9	18.9
Dihedral angle restraints	0.2 ± 0.2	0.03
Bond lengths	2.1 ± 0.4	2.4
Bond angles	17.4 ± 2.6	17.6
Improper angles	2.1 ± 0.4	2.2
van der Waals repulsion	4.1 ± 1.8	2.2

[a]Notation of the NMR structures is as follows: ⟨*Compstatin*⟩ is the ensemble comprising the final 21 simulated annealing structures; $\overline{Compstatin}$ is the mean structure obtained by averaging the coordinates of the individual simulated annealing structures; $(\overline{Compstatin})_r$ is the restrained regularized mean structure obtained by restrained regularization of the mean structure $\overline{Compstatin}$.

The cyclic peptide Compstatin forms a type I β-turn spanning residues Gln^5-Asp^6-Trp^7-Gly^8 (Fig. 2A, B). The general criteria

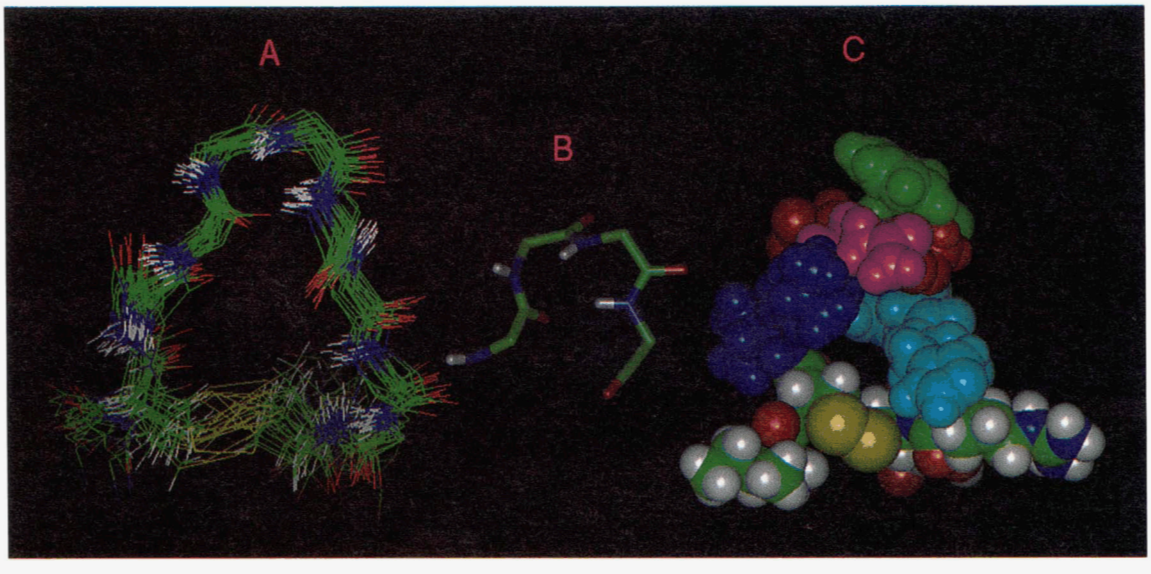

Fig. 2. A: Backbone and disulfide bond of the ensemble of the family of the final refined 21 structures of Compstatin. White denotes hydrogen; blue, nitrogen; green, carbon; red, oxygen; and yellow, sulfur. **B:** Type **I** β-turn segment of the averaged restrained regularized structure of Compstatin spanning the residues Gln^5-Asp^6-Trp^7-Gly^8. **C:** Space-filling model of Compstatin. Side-chain interactions are depicted between Val^3 and Val^4 (blue), Gln^5 (magenta), Trp^7 (green), Asp^6 and Gly^8 (red), and His^9 and His^{10} (cyan). The disulfide bond is shown in yellow. The rest of the residues are colored with the standard atomic color code for hydrogens (white), nitrogens (blue), carbons (green), and carbonyl oxygens (red).

for the presence of a β-turn are: a $C^{\alpha}(1)$–$C^{\alpha}(4)$ distance <7 Å and that the central residues are not helical (Chou & Fasman, 1977; Schulz & Schirmer, 1979; Rose et al., 1985; Wilmot & Thornton, 1988). The presence of a C=O(1)−HN(4) hydrogen bond is possible, but not necessary for stabilization of the β-turn (Chou & Fasman, 1977). More specifically, a type I β-turn is characterized by dihedral angles $(\phi_2,\psi_2) = (-60°,-90°)$ and $(\phi_3,\psi_3) = (-90°,0°)$ (Venkatachalam, 1968; Richardson, 1981; Rose et al., 1985; Wilmot & Thornton 1988). Table 2 compares the characteristic dihedral angles and distances for the Type I β-turn of Compstatin with the classic type I β-turn.

Type I β-turns are the most abundant turns in protein and peptide structures, and they are two to three times more common than any of the other major categories, the type II or type III turns; the rest are very rare (Schulz & Schirmer, 1979; Wilmot & Thornton, 1988). Position 4 of the Compstatin β-turn is occupied by Gly, which has been found to be by far the most favorable amino acid in the fourth position of a type I turn (Wilmot & Thornton, 1988). Likewise, position 2 of the β-turn of Compstatin is occupied by Asp, which has been found to be one of the most favorable amino acids in type I β-turns (Wilmot & Thornton, 1988).

Figure 2C shows a space-filling model of the average restrained regularized structure of Compstatin. Long-range spatial contacts of the rings of His^9 and Trp^7 with Gly^8, Gln^5, and Asp^6 and of the methyls of Val^3 and Val^4 with Gln^5 and Asp^6 are consistent with observed NOEs. A clustering of hydrophobic side chains of Val^3, Val^4, and Trp^7 was observed. Calculation of the solvent-accessible area (Lee & Richards, 1971) of Compstatin revealed reduced solvent accessibility for residues Gln^5 and Gly^8 at the two ends of the β-turn. This is probably the effect of capping of the turn by the rings of Trp^7 because of hydrophobic clustering toward the side chains of Val^3 and Val^4. Also, reduced surface accessibility was observed at Cys^2 and Cys^{12}, presumably because of restriction of the side chains by the disulfide bond.

Consistency of the calculated structures with the NMR parameters

There are several direct NMR criteria for the detection of β-turns, such as characteristic NOE connectivities, $^3J_{NH\text{-}H\alpha}$-coupling constants, temperature coefficients, and chemical shifts (Wüthrich, 1986; Dyson et al., 1988; Dyson & Wright, 1991, 1995). However, in several instances, the presence of multiple peptide conformers can produce an averaging of the NMR parameters that can hinder a straightforward analysis (Dyson et al., 1988). In these cases, the NMR parameters, alone and in the absence of a complete structure calculation, might not be sufficient to detect classical β-turns, but they should be consistent with the definition of a particular turn type (Wüthrich, 1986). The consistency of the measured NMR parameters with the calculated average structure of Compstatin is discussed below.

In general, the NOEs that are consistent with the presence of β-turns are NH(2)-NH(3), NH(3)-NH(4), $H^{\alpha}(2)$-NH(3), $H^{\alpha}(3)$-NH(4), and $H^{\alpha}(2)$-NH(4) (Wüthrich, 1986). In the case of an ideal type I β-turn, strong NH(2)-NH(3) (corresponding to a distance of 2.6 Å), NH(3)-NH(4) (2.4 Å), medium $H^{\alpha}(2)$-NH(3) (3.4 Å), $H^{\alpha}(3)$-NH(4) (3.2 Å), and weak $H^{\alpha}(2)$-NH(4) (3.6 Å) NOEs are observed. NOEs that distinguish a type I from a type II β-turn are: a strong NH(2)-NH(3) NOE (2.6 Å) and a medium $H^{\alpha}(2)$-NH(3) NOE (3.4 Å) in an ideal type I β-turn, as opposed to a weak NH(2)-NH(3) NOE (4.5 Å) and a strong $H^{\alpha}(2)$-NH(3) NOE (2.2 Å) in an ideal type II turn. In the case of Compstain, a strong NH(3)-NH(4) (compared to other NH-NH) NOE was observed between Trp^7 and Gly^8, a finding that is therefore consistent with the presence of a β-turn (type I or II). A strong NH(2)-NH(3) NOE was observed between residues Asp^6 and Trp^7, indicating the presence of a type I β-turn. The other characteristic of a type I β-turn, a medium $H^{\alpha}(2)$-NH(3) NOE between Asp^6 and Trp^7, could not be assigned unambiguously because of overlap with the strong intraresidue Trp^7 NH-H^{α} NOE (the H^{α} of Asp^6 and Trp^7 were at 4.56 and 4.57 ppm, respectively). Increasing the temperature from 5 °C to 10 °C did not resolve this ambiguity because of the small effect of temperature on α-protons. Finally, for a similar reason, the $H^{\alpha}(2)$-NH(4) weak NOE between Asp^6 and Gly^8 could not be distinguished from the medium $H^{\alpha}(3)$-NH(4) NOE between Trp^7 and Gly^8. More specifically, a medium NOE at (H^{α}, NH) = (4.57, 8.47) ppm was observed, which most likely corresponds to the medium expected $H^{\alpha}(3)$-NH(4) NOE between Trp^7 and Gly^8 (characteristic of a β-turn). This NOE hinders the unambiguous assignment of the expected weak $H^{\alpha}(2)$-NH(4) NOE between Asp^6 and Gly^8 (also characteristic of a β-turn). This is due to the overlap of the H^{α}-resonances of Asp^6 and Trp^7. The temperature increase to 10 °C did not resolve this ambiguity. However, an $H^{\beta}(2)$-NH(4) very weak NOE between Asp^6 and Gly^8 was observed in the 200-ms NOESY spectrum; this NOE gained significant intensity in the 400-ms NOESY spectrum, where some degree of spin diffusion is present.

In addition to NOEs, $^3J_{NH\text{-}H\alpha}$-coupling constants can be used to validate the presence of a β-turn (Wüthrich, 1986). However, $^3J_{NH\text{-}H\alpha}$-coupling constants should only be used in a qualitative

Table 2. *Criteria for the formation of a Type I β-turn*[a]

	ϕ_2	ψ_2	ϕ_3	ψ_3	$C^{\alpha}(1)$-$C^{\alpha}(4)$	C=O(1)−N(4)
Classic Type I β-turn	−60° ± 30°	−30° ± 30°	−90° ± 30°	0° ± 30°	<7 Å	2–5 Å
⟨Compstatin⟩ Type I β-turn[b]	−65° ± 13°	−26° ± 8°	−108° ± 12°	−14° ± 3°	4.7 ± 0.2 Å	3.3 ± 0.4 Å
$(\overline{\text{Compstatin}})_r$ Type I β-turn	−76°	−23°	−100°	−14°	4.8 Å	3.4 Å

[a]Notation for the Compstatin structures is as in Table 1.
[b]Compstatin β-turn spans the segment Gln^5-Asp^6-Trp^7-Gly^8.

and relative way in NMR structural analysis of peptides. This is not only because of the difficulty in measuring and interpreting $^3J_{NH\text{-}H\alpha}$-coupling constants from NMR data, but also because of conformational averaging. Absence of any $^3J_{NH\text{-}H\alpha} < 6$ Hz suggests that Compstatin is quite flexible and possibly exists in a conformational equilibrium between helical and extended dihedral angle space. $^3J_{NH\text{-}H\alpha}$-coupling constant values of $^3J_{NH\text{-}H\alpha}(2) \approx 4$ Hz and $^3J_{NH\text{-}H\alpha}(3) \approx 9$ Hz are consistent with the presence of a type I β-turn and help to distinguish a type I from a type II β-turn [the latter having $^3J_{NH\text{-}H\alpha}(3) \approx 5$ Hz] (Wüthrich, 1986). In the case of Compstatin, a small $^3J_{NH\text{-}H\alpha}(2)$-coupling constant for Asp^6 relative to a large $^3J_{NH\text{-}H\alpha}(3)$-coupling constant for Trp^7 was observed (see Supplementary material in the Electronic Appendix), another finding that is consistent with the presence of a type I β-turn.

$^3J_{NH\text{-}H\alpha}$-coupling constants have been used to evaluate the population of the β-turn conformer in peptides, on the basis of the $^3J_{NH\text{-}H\alpha}$-value of residue 2 of the β-turn (Campbell et al., 1995). The averaging of $^3J_{NH\text{-}H\alpha}(2)$ reflects the presence of an equilibrium between different structural conformers. Assuming a two-state model of a β-turn and an extended conformation, a 100% β-turn conformer corresponds to $^3J_{NH\text{-}H\alpha}(2) = 4$ Hz (or $\phi_2 = -60°$) and a 100% extended conformer corresponds to $^3J_{NH\text{-}H\alpha}(2) = 9$ Hz (or $\phi_2 < -100°$). Using this model and a $^3J_{NH\text{-}H\alpha}(2) = 6.9$ Hz for Asp^6 at position 2 of the β-turn [$^3J_{NH\text{-}H\alpha}$ extracted with the method of Kim and Prestegard (1989)], we calculated a population for a β-turn conformation of 42%. If we take into account an estimated error of 1 Hz in measuring $^3J_{NH\text{-}H\alpha}$-coupling constants and the fact that the $^3J_{NH\text{-}H\alpha}$-coupling constants extracted from DQF-COSY spectra might represent an upper limit of the actual $^3J_{NH\text{-}H\alpha}$-value (see Supplementary material), we estimate that a β-turn population of 42–63% is present in the case of Compstatin.

Deviations of observed chemical shifts from random coil values are indicative of the presence of secondary structure. For α-protons, a mean difference of -0.39 ppm or of $+0.37$ ppm is indicative of a helical or an extended conformation, respectively (Wishart et al., 1991). No α-proton chemical shift difference greater than ± 0.3 ppm was observed for Compstatin. Thus, it appears that there is no strong preference for a helical or extended conformation and that Compstatin is found in a rather flexible conformational environment. In addition, temperature-dependent experiments did not reveal a preference for hydrogen bonding for the NH of Gly^8 (residue 4 of the β-turn).

Biological significance and structural determinants important in compstatin-C3 binding

Complement-mediated pathology has been reported in several diseases; thus, a specific complement inhibitor of therapeutic value needs to be developed. However, none is currently available. It is well known that activation of one pathway (classical or alternative or lectin) leads to recruitment of another. For example, activation of the classical pathway results in the activation of the alternative pathway (Meri & Pangburn, 1990). Similarly, activation of the lectin pathway supports the activation of the alternative pathway (Reid & Turner, 1994; Matsushita, 1996). Thus, in most clinical conditions, multiple pathways are activated. These results suggest the usefulness of a complement inhibitor that blocks all three pathways. The three pathways converge at the C3 activation step; therefore, blocking this step would result in total shut-off of the complement cascade, including generation of C3a and C5a and MAC formation. In fact, many physiological regulators of complement, e.g., factor H, CR1, DAF, and MCP, act on C3b to inhibit complement activation. A soluble form of CR1 has been tested and found to suppress complement pathology in a number of in vivo complement-dependent diseases models (Kalli et al., 1994). However, identifying a smaller biologically active fragment of these regulatory proteins or a peptide mimetic is necessary for structural studies and the rational design of a clinical drug.

In our previous study, we have isolated and functionally characterized a small cyclic C3-binding peptide, Compstatin, that is a potent inhibitor of complement (Sahu et al., 1996). In the present study, in order to identify the residues essential for Compstatin interaction with C3, we have synthesized an 11-residue peptide that has the sequence of Compstatin, except for Ile^1 and Thr^{13}, and also generated nine Ala mutants in which each amino acid between Cys^2 and Cys^{12} was replaced (we followed the notation of Compstatin after sequence alignment). Replacement of Val^4, His^9, His^{10}, and Arg^{11} resulted in minimal change in the functional activity, suggesting that these residues do not contribute significantly to binding with C3 (Table 3). Replacement of Val^3, Gln^5, Asp^6, and Trp^7 reduced the activity of the peptide by 6–36-fold. Replacing Gly^8 dramatically reduced the activity of the peptide by more than 100-fold. It is interesting that four of these five residues comprise the type I β-turn of Compstatin. The calculated type I β-turn segment (Gln^5-Asp^6-Trp^7-Gly^8) is important in preserving the conformational stability of Compstatin and probably plays a significant role in the inhibitory activity. The total loss of biological activity that resulted from replacement of Gly^8 is probably related to loss of the turn structure. Given the amino acid composition of the turn, Gly^8 might be needed to release the steric hindrance and stabilize the turn structure. Of the four residues that comprise the type I β-turn, it seems that the two end residues, Gln^5 and Gly^8, which are somehow buried (as demonstrated by the solvent accessibility calculation), are more essential for Compstatin activity. However, the role of Val^3 in peptide binding is not obvious. As discussed above, a hydrophobic clustering of the side chains of Val^3, Val^4, and Trp^7 is present in Compstatin. Interaction of the side chain of Val^3 with Gln^5 and Asp^6 are observed in the calculated structure. These interactions might be important in stabilizing the β-turn. The same residues that are involved in side-chain and backbone interactions that stabilize the β-turn are also important for the functional activity of Compstatin. It is possible that disruption of the turn structure can cause loss of inhibitory activity of Compstatin. Further studies examining the structure of the five Ala mutants that significantly decrease the inhibitory activity of Compstatin (see above) are underway.

The possibility that Compstatin undergoes structural reorientation upon binding is open, and studies of the bound peptide are planned. A comparison between the structures of the free and the bound peptide could yield significant insight into the C3–peptide recognition process.

Peptide conformational changes upon binding have been observed by NMR spectroscopy, with a most common case that of the cyclophilin–cyclosporine complex (Weber et al., 1991; Wüthrich et al., 1991). In the case of cyclosporine complexed to cyclophilin, inversion of the orientation of the dominant hydrophobic cluster and the peptide backbone, together with the presence of intermolecular hydrogen bonding, have been shown to be important for recognition and binding (Weber et al., 1991; Wüthrich et al., 1991). Likewise, it has been suggested recently that, during the regulation of apoptosis, the Bcl-x_L receptor protein undergoes structural re-

Table 3. *Amino acid sequence, mass spectral analysis, and complement inhibitory activities of Compstatin (Peptide I) and its analogues*

Peptide	Amino acid sequence[a]	Mass spectral analyses		Inhibition of complement activity[b]
		Expected	Observed	IC_{50} (μM)
Peptide I	I*CVVQDWGHHRC*T	1,552	1,551	12
Peptide II	ICVVQDWGHHRCT	1,660	1,664	>600
Peptide III	*CVVQDWGHHRC*	1,340	1,339	33
Peptide IV	*CAVQDWGHHRC*	1,311	1,309	1,200
Peptide V	*CVAQDWGHHRC*	1,311	1,309	67
Peptide VI	*CVVADWGHHRC*	1,282	1,281	910
Peptide VII	*CVVQAWGHHRC*	1,296	1,297	257
Peptide VIII	*CVVQDAGHHRC*	1,224	1,223	182
Peptide IX	*CVVQDWAHHRC*	1,353	1,352	>1,200
Peptide X	*CVVQDWGAHRC*	1,273	1,272	15
Peptide XI	*CVVQDWGHARC*	1,273	1,272	74
Peptide XII	*CVVQDWGHHAC*	1,254	1,255	70

[a]Asterisks denote oxidized cysteines.
[b]Alternative pathway complement activity was measured by Er lysis assay as described in Materials and methods.

orientation to expose a hydrophobic segment upon binding of the Bak peptide (Sattler et al., 1997). The hydrophobic cluster of Compstatin might be mediating hydrophobic interactions with C3 through its binding site. The presence of a negative charge in Asp^6 at the second position of the β-turn and the possible role of this residue in charge–charge interactions during binding, together with hydrogen bonding possibilities involving the side chains of Gln^5 and Asp^6, are important subjects for further investigation.

Materials and methods

Peptide synthesis, purification, and characterization

Compstatin (peptide I) and its analogues (peptides II–XI) were synthesized in an Applied Biosystem peptide synthesizer (model 431A) using Fmoc amide resin. The side-chain protecting groups were: Cys(Trt), Asp(otBu), Arg (Pmc), Thr (tBu), Gln (Trt), Trp-(Boc), His(Trt). All peptides were cleaved from the resin by incubation for 3 h at 22 °C with a solvent mixture containing 5% phenol, 5% thioanisole, 5% water, 2.5% ethanedithiol, and 82.5% TFA. The reaction mixture was filtered through a fritted funnel, precipitated with cold ether, dissolved in 50% acetonitrile containing 0.1% TFA, and lyophilized. The crude peptides obtained after cleavage were dissolved in 10% acetonitrile containing 0.1% TFA and purified using a reversed-phase C-18 column (Waters, Milford, Massachusetts). Disulfide oxidation of all the purified peptides was performed by stirring a 0.15 mM solution of the peptide in 0.1 M ammonium bicarbonate, pH 8.0, and bubbling with oxygen at 22 °C for 48 h. Purified peptide II was reduced and alkylated with 10 mM dithiothreitol and 40 mM iodoacetamide. The purity and identity of Compstatin and its analogues were critically monitored by analytical chromatography and laser desorption mass spectrometry (Moore, 1993). Formation of a disulfide bond in each cyclic peptide was confirmed by mass spectrometry using a mass shift assay that involves reaction of thiols with *p*-hydroxy mercuribenzoic acid (Angeletti et al., 1996).

Complement inhibition assay

Inhibition of complement function by Compstatin and analogue peptides was studied by measuring their effect on the alternative pathway of complement. Inhibition of complement activation was determined by measuring the lysis of rabbit erythrocytes (Er) in normal human serum as described previously (Sahu & Pangburn, 1996). Various concentrations of peptide were mixed with 5 μL of NHS, 5 μL of 0.1 M MgEGTA, and 10 μL of Er (1×10^9/mL) and brought to a final volume of 100 μL in GVB (5 mM barbital, 0.1% gelatin, and 145 mM NaCl, pH 7.4). The reaction mixture was incubated at 37 °C for 20 min and stopped by adding 200 μL of GVBE (GVB with 10 mM EDTA). After centrifugation, lysis of Er was determined at 414 nm. The percentage of lysis obtained was normalized by considering 100% lysis to be equal to the lysis occurring in the absence of the peptide. The concentration of the peptide causing 50% inhibition of hemolytic activity was taken as the IC_{50}.

NMR sample preparation

The NMR samples were prepared by dissolving Compstatin in 0.6 mL of 90% H_2O/10% D_2O containing 0.05 M potassium phosphate, 0.1 M potassium chloride, 0.1% sodium azide, and 10^{-5} M EDTA. Compstatin is highly soluble in aqueous solution; solvation to a final concentration of 3 mM was instantaneous. Mass spectroscopy showed the solution to be monomeric. The sample, prepared at pH 6, was highly pure and suitable for NMR spectroscopy. pH 6 was chosen because it is lower than the pH favoring cysteine oxidation–reduction reactions and higher than that favoring hydrolysis at the aspartic acid position. This pH was sufficient to achieve slow amide proton exchange with the solvent in order to facilitate the proton assignments. As assessed by mass spectroscopy and 1D NMR spectra, the sample was stable over the period of several days required to collect the 2D NMR spectra. Most experiments were performed at 5 °C to slow down the peptide tumbling time and to limit potential exchange between the various peptide conformers and amide proton exchange with the solvent.

NMR data acquisition

NMR spectra of Compstatin were acquired with a Varian Unity-plus 500 MHz spectrometer. Standard methods were used to obtain 1D and 2D ^{1}H NMR spectra. These included 2D TOCSY (Braunschweiler & Ernst, 1983), 2D DQF-COSY (Rance et al., 1983), 2D DQ (Braunschweiler et al., 1983), 2D NOESY (Kumar et al., 1980), 2D J-R NOESY (Plateau & Guéron, 1982), and ROESY (Bothner-By et al., 1984). Experiments were performed at 5 °C and some were repeated at 10 °C. Experimental constraints for structure calculations were extracted from the 5 °C spectra. Mixing times were 150, 200, and 400 ms for the NOESY, 200 ms for the J-R NOESY, 60 ms for the TOCSY, and 150 ms for the ROESY experiments. The excitation period for the DQ experiments was 40 ms.

Conversion of NMR parameters to structural restraints

Cross peak volume integrations were performed with the program FELIX 2.3, using mainly the 150-ms 2D NOESY experiment collected at 5 °C. The NOE volumes were then converted to distance restraints after they were calibrated using known fixed distances of the Trp^7 ring. The cross peaks corresponding to NH$^\epsilon$-CH$^\delta$ and NH$^\epsilon$-CH$^{\zeta 2}$ NOEs of Trp^7 were used as reference for the calibration within the program FELIX 2.3. Then an NOE restraint file was generated with four distance classifications, as follows: strong NOEs (1.8 Å $\leq r_{ij} \leq$ 2.7 Å, where 1.8 Å is the van der Waals radius and r_{ij} is the interproton distance between protons i, j), medium NOEs (1.8 Å $\leq r_{ij} \leq$ 3.3 Å), weak NOEs (1.8 Å $\leq r_{ij} \leq$ 5.0 Å), and very weak NOEs (3.0 Å $\leq r_{ij} \leq$ 6.0 Å). The upper boundary of NOEs involving amide protons was extended to 2.9 Å for strong NOEs and to 3.5 Å for medium NOEs to account for the higher observed intensity of this type of cross peak (Qin et al., 1996). In addition, a 0.5-Å correction (Qin et al., 1996) was added to the upper boundary of the distances involving methyl groups to account for the averaging of the three methyl protons. An NOE restraint between the two sulfur atoms of Cys^2 and Cys^{12} was set during the distance geometry calculation, corresponding to distance 2.02 Å. During structure calculations, distances involving nonstereospecifically assigned or degenerate methylene protons and methyl groups were incorporated as $(\Sigma r^{-6})^{-1/6}$ effective distances (Nilges, 1993). A total of 136 NOE-derived distance restraints were used, 83 intraresidue, 30 backbone–backbone or H$^\beta$-backbone, and 23 medium- and long-range, corresponding to an average of 10.5 NOEs per residue.

Resolved β-methylene protons were observed only for residues His^9, Arg^{11}, and Cys^{12}. Resolved methyl protons were observed for residues Ile^1 and Val^4. Stereospecific assignments were made for the β-methylene protons of His^9 and Cys^{12}. Side-chain χ_1-dihedral angles for the residues involving stereospecific β-methylene proton assignments were restrained to one of the staggered conformations. In the case of His^9 and Cys^{12}, the value was found to be $\chi_1 = -60 \pm 30°$, using the combined information from H$^\alpha$-H$^\beta$ DQF-COSY cross peak patterns and NOE intensities of NH-H$^\beta$ cross peaks.

$^3J_{\text{HN-H}\alpha}$-coupling constants were measured from the 2D DQF-COSY spectrum using the method of Kim and Prestegard (1989). For accurate evaluation of coupling constants, the data were processed without window function weighting, and they were zero filled to 16K points in the t_2-dimension. The $^3J_{\text{NH-H}\alpha}$-coupling constant of Cys^2 was estimated from the 1D ^{1}H NMR spectrum. The $^3J_{\text{NH-H}\alpha}$-coupling constants corresponded to all residues except Ile^1. The calculated coupling constants and their estimated error of 1 Hz were used for direct J-coupling refinement in the final stages of the peptide structure calculation.

Dihedral angles were calculated using the J-values extracted by solving the Karplus equation (Karplus, 1959; Bystrov, 1976) with coefficients $A = 6.98$, $B = -1.38$, $C = 1.72$ (Wang & Bax, 1996). Only ϕ-angles that correspond to $^3J_{\text{NH-H}\alpha}$-coupling constants that yielded only two real roots for ϕ when solving the Karplus equation (Karplus, 1959) were used. Specifically, for $^3J_{\text{NH-H}\alpha} \geq 9$ Hz, a dihedral angle of $\phi = -120 \pm 40°$ was used and for $7.9 \leq {}^3J_{\text{NH-H}\alpha} < 9$ Hz, a dihedral angle of $\phi = -120 \pm 50°$ was used. The range was calculated to be ±20° and ±30° for the two categories, respectively, in order that both solutions of the Karplus equation would be covered with an additional ±20° as an error. For $^3J_{\text{NH-H}\alpha} \leq 7.3$ Hz, no ϕ-angle restraint was used, because all four solutions of the Karplus equation are possible for a turn segment. However, during the direct $^3J_{\text{NH-H}\alpha}$-coupling constant minimization, we used all evaluated $^3J_{\text{NH-H}\alpha}$-coupling constants and no ϕ-angle restraint.

A total of 7 (of 12 calculated) ϕ-dihedral angle, 2 χ_1-dihedral angle, and 12 $^3J_{\text{NH-H}\alpha}$-coupling constant restraints were used. The 7 ϕ-angles used corresponded to Cys^2, Val^3, Trp^7, His^9, His^{10}, Cys^{12}, and Thr^{13}.

Structure calculations

The Compstatin structures were calculated using the hybrid distance geometry-simulated annealing and refinement protocol (Nilges et al., 1988; Kuszewski et al., 1992), with further direct $^3J_{\text{NH-H}\alpha}$-coupling refinement (Garrett et al., 1994) using the program X-PLOR 3.851 (Brünger, 1992). The minimized target function during simulated annealing was composed of quadratic harmonic potential terms for covalent geometry (bonds, angles, planes, chirality), a quartic van der Waals repulsion term for the nonbonded contacts, quadratic square-well potentials for the experimental distance and dihedral angle restraints, and harmonic potential for the $^3J_{\text{NH-H}\alpha}$-coupling constant restraints (Brünger, 1992; Garrett et al., 1994). No hydrogen bonding, electrostatic, or 6-12 Lennard-Jones empirical potential energy terms were present in the simulated-annealing target function. A standard quadratic target function was minimized during distance geometry (Brünger, 1992).

The input force constants for bonds, angles, planes, and chirality were 1,000 kcal mol^{-1} Å^{-2}, 500 kcal mol^{-1} rad^{-2}, 500 kcal mol^{-1} rad^{-2}, and 500 kcal mol^{-1} rad^{-2}, respectively, and 4 kcal mol^{-1} Å^{-4} for the quartic van der Waals repulsion term. The input NOE, dihedral angle, and $^3J_{\text{HN-H}\alpha}$-coupling constant force constants were 50 kcal mol^{-1} Å^{-2}, 200 kcal mol^{-1} rad^{-2}, and 1 kcal mol^{-1} Hz^{-2}, respectively. Force constants were varied during the various steps of the structure calculation according to the standard X-PLOR protocols (Brünger, 1992).

A total of 100 structures were generated, and those with low energies and with no NOE violation >0.3 Å, no dihedral angle violation >5°, no bond violation >0.05 Å, no angle violation >5°, and no improper angle violation >5° were accepted. The accepted NOE and dihedral angle refined structures were then subjected to further minimization using NOE, χ_1-dihedral angle, and $^3J_{\text{NH-H}\alpha}$-coupling constant restraints, but not ϕ-dihedral angle restraints. This procedure was repeated iteratively to evaluate more distance restraints. A family of structures with similar geometries in the Gln^5–Gly^8 region was observed and the best structure with low-

energy terms and no $^3J_{NH\text{-}H\alpha}$-coupling constant violation >1.2 Hz was selected for further final refinement.

Coordinates

Coordinates have been deposited with the Brookhaven National Protein Data Bank (code 1a1p).

Supplementary material in electronic appendix

We have included an Electronic Appendix that contains details relevant to $^3J_{NH\text{-}H\alpha}$-coupling constant evaluation (Fig. 1), structure calculation and solvent accessibility (Fig. 2), and chemical shift analysis (Fig. 3). ^{1}H NMR chemical shifts of Compstatin are given in Table 1. The coordinates of the average restrained regularized structure of Compstatin are given in the file acst.pdb.

Acknowledgments

We thank Dr. William T. Moore for his helpful suggestions, Dr. Xin Jia and Lynn Spruce for their excellent technical assistance, and Dr. Deborah McClellan for editorial assistance. This research was supported by National Institute of Health Research grant AI 30040 and Cancer and Diabetes Centers Core Support grants CA 16520 and DK 19525. The work at The Burnham Institute was supported by a core grant NIH 5 P30-CA30199 and Lucille Markey Foundation grants to La Jolla Cancer Research Foundation.

References

Angeletti RH, Bibbs L, Bonewald LF, Fields GB, McMurray JS, Moore WT, Stults JT. 1996. Formation of disulfide bond in an octreotide-like peptide: A multicenter study. In: Marshak DR, ed. *Techniques in protein chemistry VII.* San Diego, California: Academic Press. p 261.

Bothner-By AA, Stephens RL, Lee JM, Warren CD, Jeanloz RW. 1984. Structure determination of a tetrasaccharide: Transient nuclear Overhauser effects in the rotating frame. *J Am Chem Soc 106*:811–813.

Braunschweiler L, Bodenhausen G, Ernst RR. 1983. Analysis of networks of coupled spins by multiple quantum NMR. *Mol Phys 48*:535–560.

Braunschweiler L, Ernst RR. 1983. Coherence transfer by isotropic mixing: Application to proton correlation spectroscopy. *J Magn Res 53*:521–528.

Brünger AT. 1992. *X-PLOR version 3.1.* New Haven, Connecticut: Yale University Press. [http://pauli.csb.yale.edu]

Bystrov VF. 1976. Spin–spin coupling and the conformational states of peptide systems. *Prog Nucl Magn Res Spectrosc 10*:41–80.

Campbell AP, McInnes C, Hodges RS, Sykes BD. 1995. Comparison of NMR solution structures of the receptor binding domains of *Pseudomonas aeruginosa* pili strains PAO, KB7, and PAK: Implications for receptor binding and synthetic vaccine design. *Biochemistry 34*:16255–16268.

Chou PY, Fasman GD. 1977. β-Turns in proteins. *J Mol Biol 115*:135–175.

Dyson HJ, Rance M, Houghten RA, Lerner RA, Wright PE. 1988. Folding of immunogenic peptide fragments of proteins in water solution. I. Sequence requirements for the formation of a reverse turn. *J Mol Biol 201*:161–200.

Dyson HJ, Wright PE. 1991. Defining solution conformations of small linear peptides. *Annu Rev Biophys Biophys Chem 20*:519–538.

Dyson HJ, Wright PE. 1995. Antigenic peptides. *FASEB J 9*:37–42.

Ehrengruber MU, Geiser T, Deranleau DA. 1994. Activation of human neutrophils by C3a and C5a: Comparison of the effects on shape changes, chemotaxis, secretion, and respiratory burst. *FEBS Lett 346*:181–184.

Ellati SG, Dahinden CA, Church MK. 1994. Complement peptides C3a- and C5a-induced mediator release from dissociated human skin mast cells. *J Invest Dermatol 102*:803–806.

Ember JA, Sanderson SD, Taylor SM, Kawahara M, Hugli TE. 1992. Biologic activity of synthetic analogues of C5a anaphylatoxin. *J Immunol 148*:3165–3173.

Frank MM, Fries LF. 1991. The role of complement in inflammation and phagocytosis. *Immunol Today 12*:322–326.

Gallinaro R, Cheadle WG, Applegate K, Polk HCJ. 1992. The role of the complement system in trauma and infection. *Surg Gynecol Obster 174*:435–440.

Garrett DS, Kuszewski J, Hancock TJ, Lodi PJ, Vuister GW, Gronenborn AM, Clore GM. 1994. The impact of direct refinement against three-bond HN-C$^\alpha$H coupling constants on protein structure determination by NMR. *J Magn Res B 104*:99–103.

Gillinov AM, Redmond JM, Winkelstein JA, Zehr KJ, Herskowitz A, Baumgartner WA, Cameron DE. 1994. Complement and neutrophil activation during cardiopulmonary bypass: A study in the complement-deficient dog. *Ann Thorac Surg 57*:345–352.

Holers VM, Kinoshita T, Molina H. 1992. The evolution of mouse and human complement C3-binding proteins: Divergence of form but conservation of function. *Immunol Today 13*:231–236.

Hugli TE. 1990. The anaphylatoxin C3a. *Curr Topica Microbiol Immunol 153*:181–208.

Johnson BJ. 1977. Complement: A host defense mechanism ready for pharmacological manipulation? *J Pharmaceut Sci 66*:1367–1377.

Kalli KR, Hsu P, Fearon DT. 1994. Therapeutic uses of recombinant complement protein inhibitors. *Springer Semin Immunopathol 15*:417–431.

Karplus M. 1959. Contact electron-spin coupling of nuclear magnetic moments. *J Chem Phys 30*:11–15.

Kilgore KS, Friedrichs GS, Homeister JW, Lucchesi BR. 1994. The complement system in myocardial ischaemia/reperfusion injury. *Cardiovasc Res 28*:437–444.

Kim Y, Prestegard JH. 1989. Measurement of vicinal couplings from cross peaks in COSY spectra. *J Magn Res 84*:9–13.

Kumar A, Ernst RR, Wüthrich K. 1980. A two-dimensional nuclear Overhauser enhancement (2D NOE) experiment for the elucidation of complete proton–proton cross-relaxation networks in biological macromolecules. *Biochem Biophys Res Commun 95*:1–6.

Kuszewski J, Nilges M, Brünger AT. 1992. Sampling and efficiency of metric matrix distance geometry: A novel "partial" metrization algorithm. *J Biomol NMR 2*:33–56.

Lambris JD. 1990. *The third component of complement: Chemistry and biology.* Berlin: Springer-Verlag.

Lambris JD. 1993. Chemistry, biology and phylogeny of C3. [Review]. *Complement Profiles 1*:16–45.

Laskowski RA, Rullmann JA, MacArthur MW, Kaptein R, Thornton JM. 1996. AQUA and PROCHECK-NMR: Programs for checking the quality of protein structures solved by NMR. *J Biomol NMR 8*:477–486.

Lee B, Richards FM. 1971. The interpretation of protein structures: Estimation of static accessibility. *J Mol Biol 55*:379–400.

Matsushita M. 1996. The lectin pathway of the complement system. *Microbiol Immunol 40*:887–893.

Meri S, Pangburn MK. 1990. A mechanism of activation of the alternative complement pathway by the classical pathway—Protection of C3b from inactivation by covalent attachment to C4b. *Eur J Immunol 20*:2555–2561.

Moore WT. 1993. Integration of mass spectrometry into strategies for peptide synthesis. *Biol Mass Spectrom 22*:149–162.

Morgan BP. 1994. Clinical complementology: Recent progress and future trends. *Eur J Clin Invest 24*:219–228.

Muller-Eberhard HJ. 1992. Complement—Chemistry and pathways. In: Gallin JI, Goldstein IM, Synderman R, eds. *Inflammation: Basic principles and clinical correlates, 2nd ed.* New York: Raven Press.

Nilges M. 1993. A calculation strategy for the structure determination of symmetric dimers by NMR. *Proteins Struct Funct Genet 17*:297–309.

Nilges M, Clore GM, Gronenborn AM. 1988. Determination of three-dimensional structures of proteins from interproton distance data by hybrid distance geometry-dynamical simulated annealing calculations. *FEBS Lett 229*:317–324.

Pekna M, Nilsson L, Nilssonekdahl K, Nilsson UR, Nilsson B. 1993. Evidence for iC3 generation during cardiopulmonary bypass as the result of blood–gas interaction. *Clin Exp Immunol 91*:404–409.

Plateau P, Guéron M. 1982. Exchangeable proton NMR without baseline distortion, using new strong-pulse sequences. *J Am Chem Soc 104*:7310–7311.

Qin J, Clore GM, Kennedy WP, Kuszewski J, Gronenborn AM. 1996. The solution structure of human thioredoxin complexed with its target from Ref-1 reveals peptide chain reversal. *Structure 4*:613–620.

Ramachandran GN, Ramakrishnan C, Sasisekharan V. 1963. Stereo-chemistry of polypeptide chain configurations. *J Mol Biol 7*:95–99.

Rance M, Sørensen OW, Bodenhausen G, Wagner G, Ernst RR, Wüthrich K. 1983. Improved spectral resolution in COSY ^{1}H NMR spectra of proteins via double quantum filtering. *Biochem Biophys Res Commun 117*:479–485.

Robbins RA, Russ WD, Rasmussen JK, Clayton MM. 1987. Activation of the complement system in the adult respiratory distress syndrome. *Am Rev Respir Dis 135*:651–658.

Reid KBM, Turner MW. 1994. Mammalian lectins in activation and clearance mechanisms involving the complement system. *Springer Semin Immunopathol 15*:307–326.

Reynard AM. 1980. The regulation of complement activity by pharmacologic agents. *J Immunopharmacol 2*:1–47.

Richardson JS. 1981. The anatomy and taxonomy of protein structure. *Adv Protein Chem 34*:167–339.

Rose GD, Gierash LM, Smith JA. 1985. Turns in peptides and proteins. *Adv Protein Chem 37*:1–109.

Sahu AB, Kay BK, Lambris JD. 1996. Inhibition of human complement by a C3-binding peptide isolated from a phage displayed random peptide library. *J Immunol 157*:884–891.

Sahu A, Pangburn MK. 1996. Investigation of mechanism-based inhibitors of complement targeting the activated thioester of human C3. *Biochem Pharmacol 51*:797–804.

Sattler M, Liang H, Nettesheim D, Meadows RP, Harlan JE, Eberstadt M, Yoon HS, Shuker SB, Chang BS, Minn AJ, Thompson CB, Fesik SW. 1997. Structure of Bcl-xL-Bak peptide complex: Recognition between regulators of apoptosis. *Science 275*:983–986.

Schulz GE, Schirmer RH. 1979. *Principles of protein structure*. New York: Springer Verlag.

Vasthare US, Rosenwasser RH, Barone FC, Tuma RF. 1993. Involvement of the complement system in cerebral ischemic and reperfusion injury. *FASEB J 7*:A424.

Venkatachalam CM. 1968. Conformation of a system of three linked peptide units. *Biopolymers 6*:1425–1436.

Wang AC, Bax A. 1996. Determination of the backbone dihedral angles ϕ in human ubiquitin from reparametrized empirical Karplus equations. *J Am Chem Soc 118*:2483–2494.

Wang MW, Johnston PS, Wright LJ, Lim SML, White DJG. 1992. Immunofluorescent localization of pig complement component-3, regardless of the presence or absence of detectable immunoglobulins, in hyperacutely rejected heart xenografts. *Histochem J 24*:102–109.

Weber C, Wider G, von Freyberg B, Traber R, Braun W, Widmer H, Wüthrich K. 1991. The NMR structure of cyclosporine A bound to cyclophilin in aqueous solution. *Biochemistry 30*:6563–6574.

Wilmot CM, Thornton JM. 1988. Analysis and prediction of the different types of β-turn in proteins. *J Mol Biol 203*:221–232.

Wishart DS, Sykes BD, Richards FM. 1991. Relationship between nuclear magnetic resonance chemical shift and protein secondary structure. *J Mol Biol 222*:311–333.

Wüthrich K. 1986. *NMR of proteins and nucleic acids*. New York: John Wiley and Sons.

Wüthrich K, von Freyberg B, Weber C, Wider G, Traber R, Widmer H, Braun W. 1991. Receptor-induced conformation change of the immunosuppressant cyclosporin A. *Science 254*:953–954.